Modeling and Analysis of WAP Performance over Wireless Links

Humphrey Rutagemwa, *Student Member*, *IEEE*, and Xuemin Shen, *Senior Member*, *IEEE*

Abstract—In this paper, an analytical model for studying the performance behaviors of wireless application protocol (WAP) over wireless links is proposed. A Rayleigh fading channel model is used to characterize the behaviors of wireless channel. Mathematical expressions that represent the performance of WAP as a function of the protocol and the channel parameters are derived. Computer simulation results are presented to validate the analytical results. It is shown that WAP performs better in a bursty error environment than in a random error environment. The goodput of WAP can be improved by increasing the WAP packet group size, but the significance of the improvement depends on the underlying channel condition.

Index Terms—Markov channel model, performance analysis, Rayleigh fading channel, wireless application protocol.

1 Introduction

Over the last decade, the Internet has been growing tremendously as evidenced by the access demand increase at the rate of 1,000 percent per year [1]. According to the Computer Industry Almanac [2], the number of worldwide Internet users surpassed 665 million in 2002 and will continue to grow strongly in the next four years. It is forecasted that, by the year-end of 2005, the number of the Internet users will top to 1 billion. The increase of mobile user reliance on Internet services, along with advancement of portable computing devices and wireless communication networks, suggests a need for people to access the Internet from anywhere. In order to provide a seamless wireless Internet access, a proper integration of the wireline networks (Internet) and existing wireless networks (e.g., mobile cellular networks) is required. Fig. 1 shows a network architecture that extends backbone Internet services to the wireless networks. In the wireline domain, the high-speed wireline links and the core routers are used as the backbone network, whereas the servers host the contents provided to the mobile Internet users. On the wireless domain, handheld devices such as PDAs, portable PCs, smart phones, etc., are used as end-user terminals. At the wireline/wireless interface, the base stations (network controller or mobile switching center) are used to provide wireless network access points to mobile users.

The Internet has been built upon the standard set of protocols collectively known as TCP/IP (Transmission Control Protocol/Internet Protocol) suite [3]. TCP is a connection orientated transport layer protocol that provides in-order end-to-end reliable data delivery services. Due to its robustness and scalability, the TCP/IP suite has been performing well over the Internet and, therefore, is widely accepted. However, the extension of the standard TCP/IP suite to the wireless networks has some various problems. One of the problems is a significant throughput degradation of the TCP [4]. This is due to the wireless channel characteristics that violate the basic assumptions from which the TCP was developed in the first place. The unfavorable wireless channel characteristics include high bit error rate, low bandwidth, poor availability, and asymmetric behaviors of downlink (a link from base satiation to mobile host) and uplink (a link from mobile host to base station). To overcome these problems, several approaches have been proposed in the literature: modification of the existing TCP/IP suite to compensate for wireless channel impairments [5], improvement of the quality of services (QoS) offered by wireless networks, and the introduction of new sets of protocols such as Wireless Application Protocol (WAP) [6]. Modifying a widely accepted TCP/IP protocol seems to be a scalable solution, but this requires careful design to maintain backward-compatibility with existing Internet systems. Improving the QoS (e.g., allocated bandwidth per user) of existing wireless networks might reduce the user capacity or requires a new set of hardware equipments, which imply a high initial cost.

WAP is an open standard and application environment proposed by WAP Forum (WAP is now taken care by Open Mobile Alliance) [6] to enable mobile users with the digital handheld devices to access the Internet and advanced telephony services. WAP has been optimized for the mobile environment where the handheld wireless devices are limited by CPU power, memory, battery lifetime, and simple user interface, and wireless links are characterized by low bandwidth, high latency, and unpredictable availability and stability. So far, little work has been done on the performance study of WAP in terms of goodput, efficiency, etc. In this paper, an analytical model for studying the performance behaviors of WAP over wireless links is proposed. First, a Rayleigh fading channel model is used to characterize the behaviors of wireless channel. Second, a three-state Markov model, which approximates error process occurring in Rayleigh fading channel at the packet-level, is developed. Third, Markov analysis is used

• *The authors are with the Department of Electrical and Computer Engineering, University of Waterloo, Waterloo, Ontario, Canada N2L 3G1. E-mail: {humphrey, xshen}@bbcr.uwaterloo.ca.*

Manuscript received 6 Sept. 2002; revised 10 Apr. 2003; accepted 1 May 2003. For information on obtaining reprints of this article, please send e-mail to: tmc@computer.org, and reference IEEECS Log Number 4-092002.

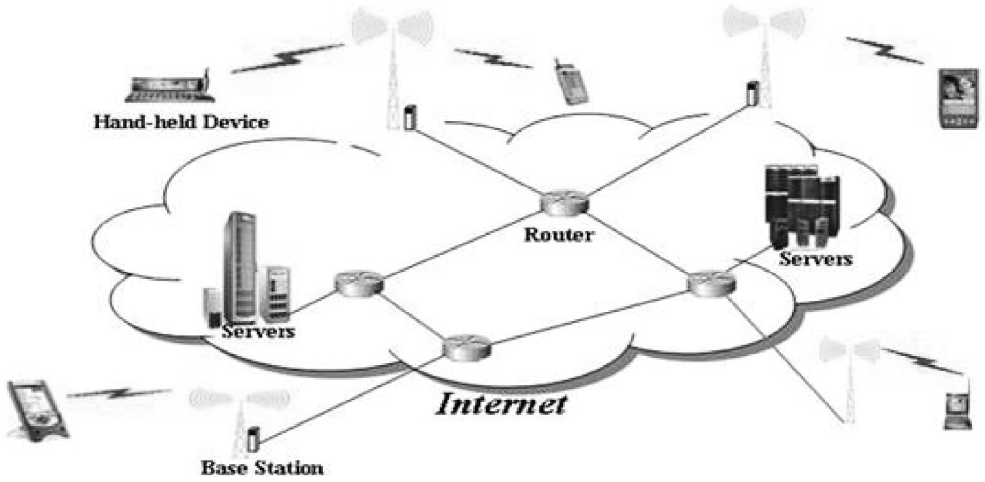

Fig. 1. Wirless Internet architecture.

to derive explicit mathematical expressions that predict the performance of WAP, in terms of goodput and efficiency, for the given channel and protocol parameters. In addition, computer simulations are carried out to validate the analytical results. The rest of this paper is organized as follows: The system models are developed in Section 2. The analysis of WAP performance is given in Section 3. Section 4 presents the simulation results, followed by concluding remarks in Section 5.

2 System Model

Fig. 2 shows a WAP wireless/Internet interworking model consisting of three types of nodes: fixed hosts (FHs), base stations (BSs), and mobile hosts (MHs). BSs are located at the wireline/wireless interface. The TCP/IP protocol is used for communication between FHs and BSs, while the WAP protocol is used for communication between BSs and MHs. In this model, WAP utilizes proxy technology to connect the wireless domain and the Internet. WAP proxy [6] (a protocol gateway which translates requests and responses between WAP protocol stack and TCP/IP protocol stack) is assumed to be hosted at the BSs. Since we are only interested in the impact of packet losses due to the wireless link, it is reasonable to assume a BS buffer is large enough such that no packet loss occurs due to congestion at the wireline/wireless interface. In general, wireline links have relatively large bandwidth and low bit error rate (BER) as compared to that of wireless links. Therefore, the end-to-end performance, in terms of throughput and efficiency, is mainly determined by the wireless links. Under this conjecture, we only concentrate on the wireless section. To study the performance behavior of WAP over a single-hop wireless link, a unidirectional traffic with error-free acknowledgement packets is considered. This assumption is acceptable since acknowledgement packets are relatively smaller in size than data packets and, therefore, a relatively lower error probability.

The WAP protocol stack is designed in a layered architecture. It has six layers: application, session, transaction, security, transport, and network layers, which are transparent from each other [6]. This study focuses on transaction layer since this layer implements and provides

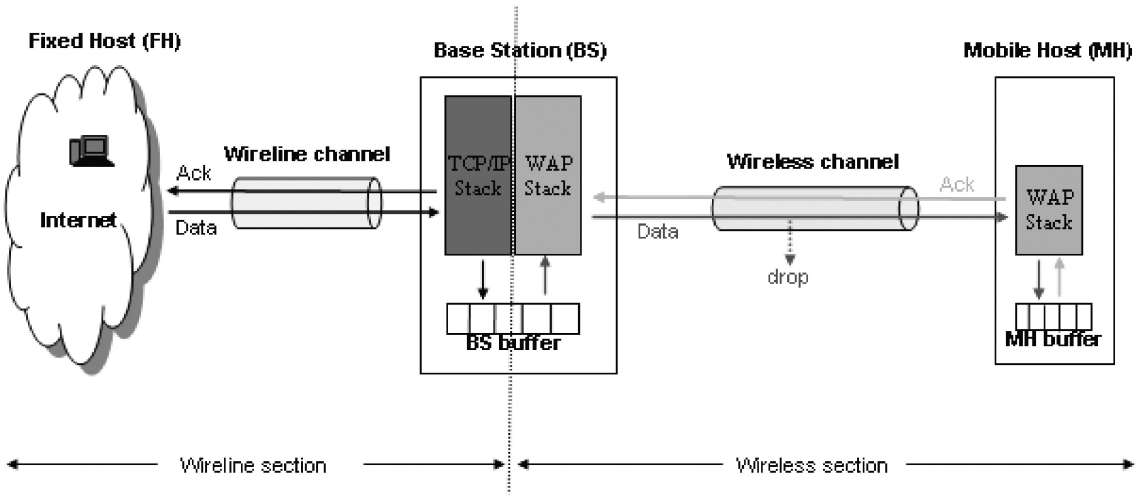

Fig. 2. Block diagram of a WAP wireless/Internet interworking model.

reliable delivery services to its above layers. To analyze the impact of wireless link on performance, WAP protocol stack is profiled into three layers: application, transaction, and network layers. The application layer generates a predefined type of data traffic, such as Web browsing like traffic, and the transaction layer reliably delivers the generated data packets over unreliable channel defined in the network layer. A class 2 Wireless Transaction Protocol (WTP) [7] is considered at the transaction layer. WTP uses group acknowledgement, selective retransmission, and timeout retransmission mechanisms to provide reliable delivery service.

For the wireless channel, a non-line-of-sight (NLOS) frequency-nonselective (flat) multipath fading channel with a packet transmission rate (in packets/seconds) much higher than the maximum Doppler frequency (Hz) is considered. The channel can be modeled as a multiplicative complex Gaussian random process $c(t)$ with zero mean and covariance function $K(\tau) = J_0(2\pi f_d|\tau|)$ [8], where $J_0(\cdot)$ is the zeroth order Bessel function of the first kind, $f_d = v/\lambda$ is the maximum Doppler frequency, v is the mobile speed and λ is the carrier wavelength. The corresponding power spectrum for the Gaussian process is given by

$$S_X(f) = \begin{cases} S_X(0)\left[1 - \left(\frac{f}{f_d}\right)^2\right]^{-1/2}, & |f| < f_d \\ 0, & otherwise. \end{cases} \quad (1)$$

The envelope $\alpha(t)$ defined as $|c(t)|$ is Rayleigh-distributed at any time t. This model has been widely accepted as it has been proven to give good predictions of measured signal statistics [8]. By considering a modulation scheme, the dynamics of the Rayleigh fading channel can be characterized at the packet level. However, the performance analysis of high-level protocols becomes quite complex. As an alternative to this problem, an approximated channel which is reasonably accurate and mathematically tractable can be developed by using a Markov model. Several Markov models have been proposed in the literature to characterize flat Rayleigh fading channels. The two-state Gilbert-Elliot model [9], [10] has been used to model bursty communication channels. In [11], [12], it has been shown that the first order Markov model, like finite-state Markov channel (FSMC) model, can accurately approximate a Rayleigh fading channel. However, when the quality of the radio channel varies dramatically, the two-state Gilbert-Elliot model becomes inadequate to present the channel dynamics. In [13], the two-state Gilbert-Elliot model is extended by proposing the modeling of Rayleigh fading channel with a FSMC model. The FSMC model is constructed by partitioning the received signal to noise ratio into a finite number of intervals and presenting each interval as a state of the Markov process. A common and simple approach for partitioning the received signal to noise ratio is to set the thresholds in such a way that steady state probabilities of being in any state are equal. However, the simple approach may not be suitable for wireless channel since more Markov states may be needed for the poorer channel condition. In this paper, thresholds are set in such a way that the probability of being in a state of higher-level doubles at each level [14]. This allocates more states in a region of higher packet error rate, and, hence, a better approximation of real channel conditions [15].

In order to develop a reasonably accurate model while minimizing the complexity of analysis, a three-state Markov channel with an improved partitioning approach is considered. A discussion for choosing a three-state Markov channel model is given in Section 3.1. The rest of this section discusses the approach used to compute the parameters of the three-state Markov channel model.

Since a received signal to noise ratio Γ is proportional to the square of the signal envelop which is Rayleigh distributed, the probability density function (p.d.f.) of Γ is exponential [16] and is given by

$$f_\Gamma(\gamma) = \begin{cases} \frac{1}{SNR}\exp(-\frac{\gamma}{SNR}), & \gamma \geq 0 \\ 0, & otherwise, \end{cases} \quad (2)$$

where SNR is the mean signal to noise ratio, defined as a ratio of average bit energy of the received signal to the noise power density. Let $0 = \Gamma_0 < \Gamma_1 < \Gamma_2 < \Gamma_3 = \infty$ be the thresholds which partition Γ such that the probability of being in a state doubles at each higher level. That is,

$$\pi_k = 2\pi_{k-1}, \text{ and } \pi_0 = \frac{1}{2^n - 1}, \quad n = 3, k = 1, 2, \quad (3)$$

where π_k and n denotes the steady-state probability and number of states, respectively. With the p.d.f. of the received signal to noise ratio given by (2), the steady-state probabilities can be obtained by

$$\pi_k = \int_{\Gamma_k}^{\Gamma_{k+1}} \frac{1}{SNR}\exp\Big(-\frac{\gamma}{SNR}\Big)d\gamma, \quad k = 1, 2. \quad (4)$$

From (4), the thresholds Γ_1 and Γ_2 can be found as

$$\Gamma_1 = -SNR\ \ln(\pi_1 + \pi_2), \quad \Gamma_2 = -SNR\ \ln(\pi_2). \quad (5)$$

With the statistical knowledge of fading channel (Rayleigh distribution in this case), analytical method [17] can be used to compute the elements of transition probability matrix $\mathbf{P}$ and the crossover probability (packet error rate) vector $\mathbf{e}$. However, the evaluation of integrals resulting from modeling the packet-level error process becomes increasingly complex. In this study, the elements of matrix $\mathbf{P}$ and vector $\mathbf{e}$ are computed from empirical data. By using a long run of sample sequence, the state transition probability matrix is estimated as

$$\mathbf{P} = [p_{ij}],\ p_{ij} = \frac{n_{ij}}{n_i},\ n_i = \sum_{j=1}^{3} n_{ij},\ i = 1, 2, 3, \quad (6)$$

where n_{ij} is the number of transitions from state i to state j. Similarly, the crossover probability vector is computed as a mean value of packet error rate over the corresponding partition interval.

3 WAP Performance Analysis

This section presents the performance analysis of a single pair WAP sender-receiver running over the wireless channel whose packet error process is modeled by the three-state Markov chain with transition probability matrix $\mathbf{P} = [p_{ij}]$ for $i, j = 1, 2, 3$ and crossover probability (packet error rate)

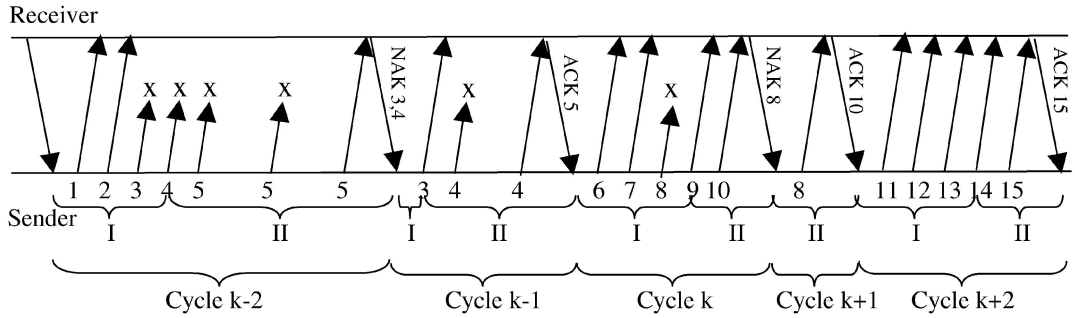

Fig. 3. Time diagram for packets transmission using WAP.

vector $\mathbf{e} = [e_i]$ for $i = 1, 2, 3$. It is assumed that channel condition remains unchanged during transmission of a packet. Therefore, it is reasonable for the state transitions of the Markov channel model to occur after every time slot (a time to transmit one packet). The metrics of interest in studying the WAP performance are goodput and efficiency. The goodput is defined as the number of packet transmitted successfully per unit time, whereas the efficiency is defined as the ratio of the number of packet transmitted successfully to the number of packet transmitted.

Fig. 3 shows a sample operation of WTP with the WAP packet group size $N = 5$. WTP protocol delivers packets in the groups. The number packets in each packet group is usually fixed and referred to as WAP packet group size or WAP group size. In the first group of transmitted packets (pkts. 1, 2, 3, 4, and 5), three packets get corrupted (pkts. 3, 4, and 5). After expiration of the timeout timer, the last packet in the group (pkt. 5) is retransmitted until it is received successfully. The WAP receiver responds with a negative acknowledgement (NAK), requesting missed packets (pkts. 3 and 4). Again, the last packet in the group (pkt. 4) is corrupted and is retransmitted after the timeout. Finally, all packets from the first group (pkts. 1, 2, 3, 4, and 5) are successfully received and WAP receiver responds with positive acknowledgement (ACK) requesting transmission of a new group of packets. A similar process continues for the subsequent groups of the packets, (pkts. 6, 7, 8, 9, and 10) and (pkts. 11, 12, 13, 14, and 15).

Consider the instances where the acknowledgement packets (NAKs or ACKs) are received and define a cycle as the time evolution between two consecutive arrivals of the acknowledgement packets. By conditioning the channel state and the number of packets remaining in the transmitted packet group at the beginning of a cycle, the transmission processes in different cycles become independent of each other. Therefore, the transmission of packets can be tracked by the random process $S(t) = (n(t), c(t-1))$, where $c(t) \in \{1, 2, 3\}$ is the state of channel at time t and $n(t) \in \{1, 2, N\}$ is the number of packets remaining in the transmitted packet group at time t. Note that t is measured in slots. By sampling the random process $S(t)$ at the beginning of every cycle (say at time t_k), a new sampled process $s(t_k)$ is a semi-Markov process with embedded Markov chain, in the state space $W_S = \{(a, i) : a \in \{1, 2, \ldots N\}, i \in \{1, 2, 3\}\}$, defined by transition probability matrix $\mathbf{\Phi} = [\phi_{(a,i)(b,j)}]$, where $\phi_{(a,i)(b,j)}$ denotes a transition probability from state (a, i) to state (b, j) for $a, b \in \{1, 2, \ldots N\}$ and $i, j \in \{1, 2, 3\}$. Note that the states $\{(N, 1), (N, 2), (N, 3)\}$ of a Markov chain $s(t_k)$ represent the instances when ACKs are received. Under the context of renewal reward process [18], these states can be considered as mark-points for the successful transmission of the previous packet group (reward) and the beginning of transmission of the new packet group (renewal).

To derive the goodput and efficiency, the transitions of embedded Markov chain $S(t_k)$ are labeled with corresponding elements of the matrices of the expected transition time $\mathbf{\Delta} = [\delta_{(a,i)(b,j)}]$ and expected number of transmitted packets $\mathbf{M} = [\boldsymbol{m}_{(a,i)(b,j)}]$. Let $Y(t)$ denote the number of packets transmitted successfully by time t. By limiting/renewal theorems [18], the long-run average goodput, λ, is given by

$$\lambda = \lim_{t\to\infty} \frac{Y(t)}{t} = \frac{N\pi_{(N,1)} + N\pi_{(N,2)} + N\pi_{(N,3)}}{\sum\limits_{(a,i)\in W_s} \pi_{(a,i)} \sum\limits_{(b,j)\in W_s} \phi_{(a,i)(b,j)}\delta_{(a,i)(b,j)}}, \quad (7)$$

where $\pi_{(N,i)}, i = 1, 2, 3$, and $\pi_{(a,i)}, (a, i) \in W_s$ are the steady-state probabilities of the Markov chain with transition matrix $\mathbf{\Phi}$ which can be found by solving the system of equations

$$\sum_{(a,i)\in W_s} \pi_{(a,i)} = 1, \ \pi_{(b,j)} = \sum_{(a,i)\in W_s} \pi_{(a,i)}\phi_{(a,i)(b,j)} \quad \forall (b, j) \in W_s. \quad (8)$$

Similarly, the long-run average efficiency, ξ, is given by

$$\xi = \lim_{t\to\infty} \frac{Y(t)}{X(t)} = \frac{N\pi_{(N,1)} + N\pi_{(N,2)} + N\pi_{(N,3)}}{\sum\limits_{(a,i)\in W_s} \pi_{(a,i)} \sum\limits_{(b,j)\in W_s} \phi_{(a,i)(b,j)}m_{(a,i)(b,j)}}, \quad (9)$$

where $X(t)$ denote the number of packet transmitted by time t.

In order to compute the elements of matrices $\mathbf{\Phi}$, $\mathbf{\Delta}$, and $\mathbf{M}$, we further consider the transmission process within a cycle in two phases: phase-I and phase-II. As shown in Fig. 3, phase-II covers the transmission process of the last packet in a cycle and phase-I covers the remainder portion of the cycle. Let $S^{(I)}(t_k)$ and $S^{(II)}(t_k)$ denote the transmission process states at the beginning of the phase-I and phase-II of a generic cycle k, respectively. Let $\mathbf{\Phi}^{(I)}$ denotes a matrix whose elements correspond to transition probability of the transmission process from state $S^{(I)}(t_k) \in W_S$ to state $S^{(II)}(t_k) \in W_S$, and $\mathbf{\Phi}^{(II)}$ denotes a matrix whose elements corresponds to transition probability of the transmission process from state $S^{(II)}(t_k) \in W_S$ to state $S^{(I)}(t_{k+1}) \in W_S$ of a

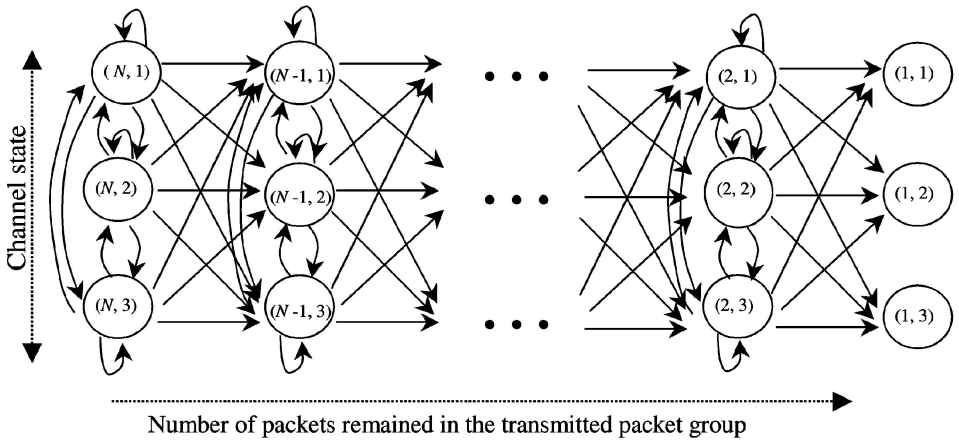

Fig. 4. State transition diagram for phase-I transmission process.

cycle $k+1$. Then, matrices $\mathbf{\Phi}$, $\mathbf{\Delta}$, and $\mathbf{M}$ can be computed by $\mathbf{\Phi} = \mathbf{\Phi}^{(I)}\mathbf{\Phi}^{(II)}$, $\mathbf{M} = \mathbf{M}^{(I)} + \mathbf{M}^{(II)}$, and $\mathbf{\Delta} = \mathbf{\Delta}^{(I)} + \mathbf{\Delta}^{(II)}$.

3.1 Analysis of Phase-I Transmission Process

Since all packets in this phase are transmitted back-to-back, the phase-I transmission process can be tracked by sampling the random process $S(t) = (n(t), c(t-1))$ in every time slot. As shown in Fig. 4, the sampled process is a Markov chain, in the state space $\{(a,i) : a \in \{1,2,...N\}, i \in \{1,2,3\}\}$, with a transition probability matrix $\mathbf{Q} = [q_{(a,i)(b,j)}]$ defined as

$$q_{(a,i)(b,j)} = \begin{cases} (1-e_i)p_{ij}, & a = b+1 \\ e_i p_{ij}, & a = b \geq 2 \\ 0, & otherwise \end{cases} \tag{10}$$

for $i,j \in \{1,2,3\}, a,b \in \{1,2,\ldots,N\}$. Note that $\mathbf{P} = [p_{ij}]$ and $\mathbf{e} = [e_i]$ for $i,j \in \{1,2,3\}$ are the Markov channel parameters.

3.1.1 Transition Probability Matrix ($\mathbf{\Phi}^{(I)}$)

Assume that the transmission process is in state (a,i) at the beginning of phase-I, the probability of the transmission process being in state (b,j) at the beginning of phase-II (i.e., transition probability after $(a-1)$ slots) is a $(a-1)$-step transition probability, computed as $\mathbf{Q}^{a-1} = [q_{(a,i)(b,j)}(a-1)]$. Therefore, the elements of the transition probability matrix $\mathbf{\Phi}^{(I)} = [\phi^{(I)}_{(a,i)(b,j)}]$ can be found as

$$\phi^{(I)}_{(a,i)(b,j)} = \begin{cases} q_{(a,i)(b,j)}(a-1), & a \geq b \\ 0, & otherwise \end{cases} \tag{11}$$

for $i,j \in \{1,2,3\}, a,b \in \{1,2,\ldots,N\}$.

3.1.2 Expected Time ($\mathbf{\Delta}^{(I)}$) and Number of Packets ($\mathbf{M}^{(I)}$)

In phase-I, all packets are transmitted back-to-back in every time slot. Therefore, the elements of matrices $\mathbf{M}^{(I)} = [m^{(I)}_{(a,i)(b,j)}]$ and $\mathbf{\Delta}^{(I)} = [\delta^{(I)}_{(a,i)(b,j)}]$ are given by

$$m^{(I)}_{(a,i)(b,j)} = \delta^{(I)}_{(a,i)(b,j)} = \begin{cases} (a-1), & a > b \\ (a-1), & b = N \\ 0, & otherwise \end{cases} \tag{12}$$

for i, $j \in \{1,2,3\}, a,b \in \{1,2,\ldots,N\}$.

3.2 Analysis of Phase-II Transmission Process

In phase-II, the last packet in a cycle is retransmitted after every round trip time $(2d+1)$ until it is transmitted successfully. The channel delay d is defined as a time taken for a packet traveling from the BS to the MH or vice-versa, which includes the propagation delay and all processing delays encountered at the end and intermediate nodes. Consider a random process $S(t) = (u(t), c(t-1))'$, where $u(t)$ represents a status of the transmitted packet in phase-II and $c(t)$ is the channel state at time t. Since phase-II covers only the transmission process of the last packet in the cycle, then the transmission process can be tracked by sampling the random process $S(t) = (u(t), c(t-1))'$ after every round trip time $(2d+1)$. As shown in Fig. 5, the sampled process is a Markov chain in the state space $\{(u,c)' : u \in \{0,1\}, c \in \{1,2,3\}\}$ (if the last packet in a cycle is transmitted successfully, then $u=0$; otherwise, $u=1$). Let $\mathbf{R}$ denotes the corresponding transition probability matrix, then $\mathbf{R} = [r_{(u,i)'(v,j)'}]$, where $r_{(u,i)'(v,j)'}$ is defined as

$$r_{(u,i)'(v,j)'} = \begin{cases} (1-e_i)p_{ij}(2d+1), & u=1, v=0 \\ e_i p_{ij}(2d+1), & u=v=1 \\ 0, & otherwise \end{cases} \tag{13}$$

for $i,j \in \{1,2,3\}, u,v \in \{0,1\}$, where $p_{ij}(2d+1)$ is the ijth entry of $(2d+1)$-step transition probability matrix $\mathbf{P}^{2d+1}$.

Since the phase-II transmission process can start in any of initial states $\{(1,1)', (1,2)', (1,3)'\}$, instantaneous transitions (dotted lines in Fig. 5), which randomly place the

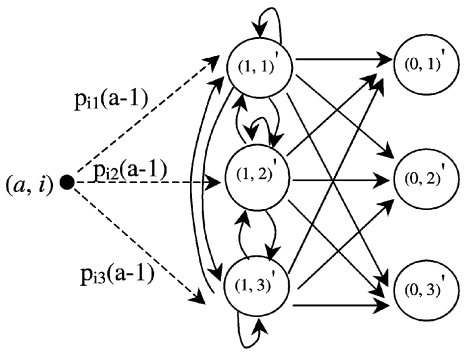

Fig. 5. State transition diagram for phase-II transmission process.

transmission process in any of transient states, are added. If the transmission process is in state $(a,i) \in W_s$ at the beginning of phase-I, the probability of transmission process being in state $(1,c)'$ at the beginning of phase-II equals to a $(a-1)$-step transition probability from the channel state i to the channel state c, i.e., $p_{i,c}(a-1)$.

3.2.1 Transition Probability Matrix ($\Phi^{(II)}$)

Let $t_{(u,i)'(v,j)'}$ denote the probability that the transmission process (see Fig. 5) will enter into the trapping state $(v,j)' \in \{(0,1)'(0,2)'(0,3)'\}$ given that the initial state is a transient state $(u,i)' \in \{(1,1)'(1,2)'(1,3)'\}$. Since all trapping states have no self-transitions, the probability matrix $\mathbf{T} = [t_{(u,i)'(v,j)'}]$ can be computed as [19]

$$\mathbf{T} = \sum_{m=0}^{\infty} \mathbf{R}^m = [\mathbf{I} - \mathbf{R}]^{-1}, \tag{14}$$

where $\mathbf{I}$ is identity matrix and $[\,]^{-1}$ denotes the inverse matrix operation. The elements of transition probability matrix $\mathbf{\Phi}^{(II)} = [\phi^{(II)}_{(a,i)(b,j)}]$ are therefore computed as

$$\phi^{(II)}_{(a,i)(b,j)} = \begin{cases} t_{(1,i)'(0,j)'}, & a = 1, b = N \\ t_{(1,i)'(0,j)'}, & a = (b+1) \\ 0, & otherwise \end{cases} \tag{15}$$

for $i,j \in \{1,2,3\}, a,b \in \{1,2,\ldots,N\}$.

3.2.2 Expected Time ($\Delta^{(II)}$) and Number of Packets ($\mathbf{M}^{(II)}$)

Let the initial state of the transmission process in Fig. 5 be $(1,i)'$. The expected number of transitions $\sigma_{(1,i)'(0,j)'}$ made in transient states $\{(1,1)', (1,2)', (1,3)'\}$ before the transmission process terminates to the final state $(0,j)'$ is given by

$$\sigma_{(1,i)'(0,j)'} = \frac{\sum_{y=1}^{3} t_{(1,i)'(1,y)'} t_{(1,y)'(0,j)'}}{t_{(1,i)'(0,j)'}} \tag{16}$$

where $\mathbf{T} = [t_{(u,i)'(v,j)'}]$ is defined by (14). The derivation of (16) is given in Appendix A. Let the transmission process be in state (a,i) at the beginning of the cycle (beginning of phase-I). By conditioning a random initial state $(1,i)'$, the expected number of transitions $\bar{\sigma}_{(a,i)(0,j)'}$ made in transient states before the transmission process terminates to the final state $(0,j)'$ is given by

$$\bar{\sigma}_{(a,i)(0,j)^{|prime}} = \frac{\sum_{x=1}^{3} p_{ix}(a-1) \sum_{y=1}^{3} t_{(1,x)'(1,y)'} t_{(1,y)'(0,j)'}}{\sum_{x=1}^{3} p_{ix}(a-1) t_{(1,x)'(0,j)'}}. \tag{17}$$

Note that, since one packet is transmitted per transition, the expected number of transitions made in transient states is equal to the expected number of packet retransmissions. Therefore, the elements of matrix $\mathbf{M}^{(II)} = [m^{(II)}_{(a,i)(b,j)}]$ are given by

$$m^{(II)}_{(a,i)(b,j)} = \begin{cases} \bar{\sigma}_{(a,i)(0,j)'}, & a > b \\ \bar{\sigma}_{(a,i)(0,j)'}, & b = N \\ 0, & otherwise \end{cases} \tag{18}$$

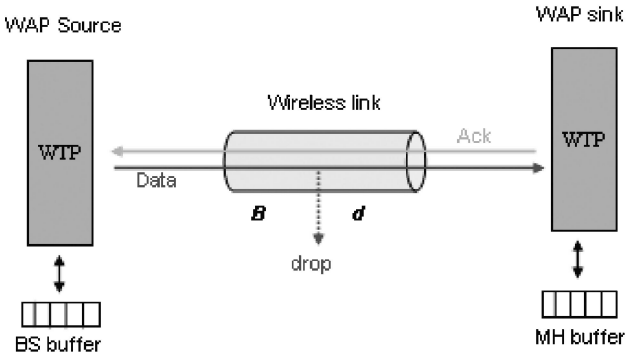

Fig. 6. Block diagram of the simulation system model.

for $i,j \in \{1,2,3\}, a,b \in \{1,2,\ldots,N\}$. Since one packet is retransmitted in every round-trip time $(2d+1)$, delay matrix $\mathbf{\Delta}^{(II)}$ can be computed as $\mathbf{\Delta}^{(II)} = (2d+1)\mathbf{M}^{(II)}$.

4 Results and Discussion

A block diagram of the simulation system model is shown in Fig. 6. A single-hop wireless link is model as a flat Rayleigh fading channel with transmission rate B and delay d. The WAP is implemented as described in Section 2 and the WAP source is set always to have data to send. MH buffer and BS buffer are considered to be sufficient large, and, therefore, WAP flow control option is not used.

The simulation is performed in two phases. In the first phase, the fading envelope is simulated by using the Jakes' method [8] and sampled after every time slot. For each sample, the corresponding packet error rate (PER) is computed by considering a BPSK (binary phase shift keying) modulation [20] and is dumped to the trace file. In the second phase, the wireless system shown in Fig. 6 is simulated at the packet level by running a single pair WAP sender-receiver over the channel whose packet error process is driven from the trace file (generated from the first phase). The evaluation of analytical results is also carried out in two phases. In the first phase, the trace file is used to compute the three-state Markov parameters as discussed in Section 2, and the second phase, the explicit equations, developed in Section 3, are used to compute the goodput and efficiency.

The analytical and simulation results are obtained by fixing transmission rate B at 64 Kbps, packet length l at 1,000 bits, carrier frequency f_c at 900 MHz, and by varying channel delay d, normalized Doppler frequency (fading rate), mean signal to noise ratio SNR, and WAP packet group size N. SNR, f_c, and fading rate are only applicable in the first phase, while d and N are only applicable in the second phase. B and l are applicable and used with the same values in both the first phase and the second phase.

4.1 Effect of the Normalized Fading Rate

Normalized fading rate (f_dT) measures how much the channel condition varies within a packet transmission time T, and, therefore, reflects the correlation of the packet errors. If the normalize fading rate is relatively small, the channel condition varies relatively slower, and, therefore, packet errors are highly correlated (bursty errors). On the other hand, if the normalize fading rate is relatively large,

TABLE 1
$\mathrm{E}[\alpha^2(t)]$, BER, PER, and L
for Deferent Values of SNR and f_dT

SNR (dB)	f_dT	$\mathrm{E}[\alpha^2(t)]$	*BER* (10^{-4})	*PER* (10^{-3})	L
10	0.016	1.00005	216.4	388.3	9.6
	0.065	1.00000	216.7	388.4	5.0
	0.260	0.99999	216.7	388.4	1.8
20	0.016	1.00005	22.8	48.2	4.7
	0.065	1.00000	22.7	47.8	1.6
	0.260	0.99999	22.7	47.8	1.1
30	0.016	1.00005	2.3	4.8	1.9
	0.065	1.00000	2.3	4.8	1.1
	0.260	0.99999	2.3	4.9	1.0

the channel varies fast, and, therefore, the packet errors occur independently (random errors). Table 1 shows the mean square of the fading envelope $\mathrm{E}[\alpha^2(t)]$, BER, PER, burst length L of the erroneous packet for various values of normalized fading rate f_dT and mean signal to noise ratio SNR. $\alpha(t)$ is the fading envelope generated by using a Jakes' method, and BER is the average bit error rate and PER is the average packet error rate. L is computed as the average number of consecutive erroneous packets. It can be seen that, as the normalized fading rate decreases, the average burst length increases. Also, it can be seen that, for a given SNR, BER, and PER remain almost unchanged as the normalized fading rate changes.

To demonstrate the accuracy of the three-state Markov channel model developed in Section 2, we compare the goodputs obtained from simulating a single pair WAP sender-receiver running over the channel whose packet error process is modeled by a two-state Markov channel model, a three-state Markov channel model, and a simulated Rayleigh fading channel. In each case, normalized fading rate is varied from 0.01 to nearly 0.3. Different values of normalized fading rate are obtained by varying the speed of mobile receiver from pedestrian speed to car speed. Other parameters are set as follows: $SNR = 15$ dB; $N = 30$; and $d = 30$ ms. From Fig. 7, it can be seen that, over a wide range of the normalized fading rate ($0.01 < f_dT < 0.3$), the three-state channel model is more accurate than the two-state channel model.

From the above analysis, the trade off between accuracy and complexity is that the two-state Markov model makes the performance analysis of the higher-level protocol relatively simple, but its accuracy in burst error environment is relatively poor. The three-state Markov model is a bit complex than the two-state Markov model, but it gives reasonably accurate results in the range of our interest ($0.01 < f_dT < 0.3$). Intuitively, four-state and higher-state Markov models are more complex and improve the accuracy than the three-state Markov model. However, the improvement in accuracy is only significant if $f_dT < 0.03$. In order to develop a reasonably accurate model for studying the performance behavior of WAP, while keeping the complexity of analysis minimum, in the range of our interest ($0.01 < f_dT < 1$), a three-state Markov model is consider.

The effect of packet loss correlation on WAP performance is studied by fixing d at 75 ms, N at 30, and by varying the normalized fading rate. Fig. 8 shows the

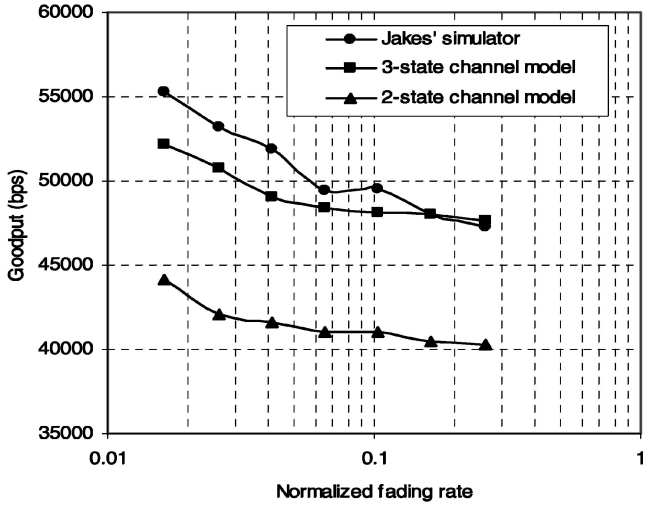

Fig. 7. Goodput versus f_dT.

simulation and analytical goodputs as a function of normalized fading rate for $SNR = 15$ dB and 25 dB. With the same parameters, Figs. 9, 10, and 11 show the corresponding number of packet loss, number of retransmission, and average NAK size, respectively.

From Fig. 8, goodput decreases as the fading rate increases for $SNR = 15$ dB and 25 dB. This indicates that WAP protocol performs better in the bursty-error (slow fading) environment than in the random-error (fast fading) environment. The slight deviations between the analytical results and the simulation results in Fig. 8 are partially due to the difference between the Jakes' method and the Markovian model (as shown in Fig. 7) and partially due to the evaluation of goodput with Markov analysis.

To understand the reason of the performance degradation in random-error environment, the number of packet losses per simulation is observed as f_dT increases. It is shown in Fig. 9 that the number of packets corrupted remains fairly constant as f_dT increases. We further examine the total number of retransmission (triggered by timeouts and NAKs) and the average number of packets

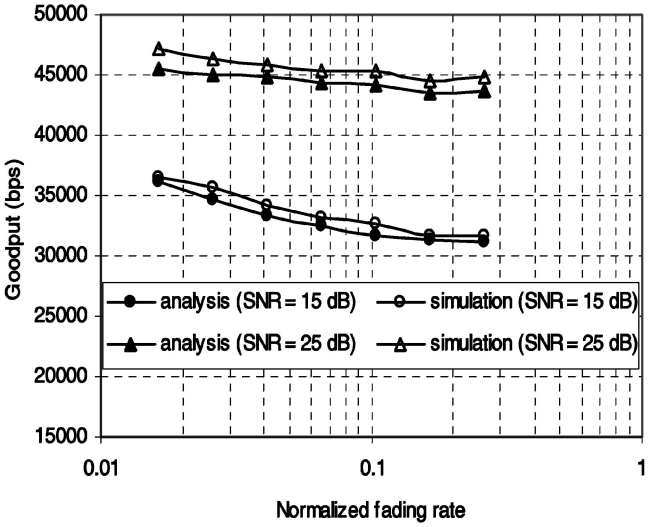

Fig. 8. Goodput versus f_dT for $SNR = 15$ dB and 25 dB.

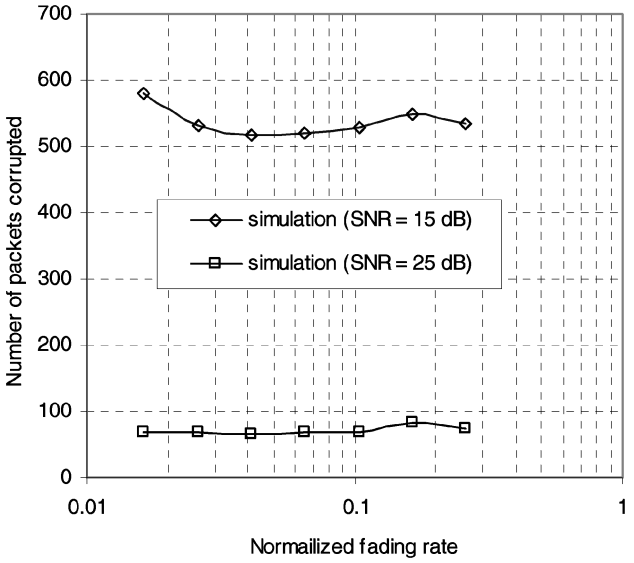

Fig. 9. Number of packet loss versus f_dT for $SNR = 15$ dB and 25 dB.

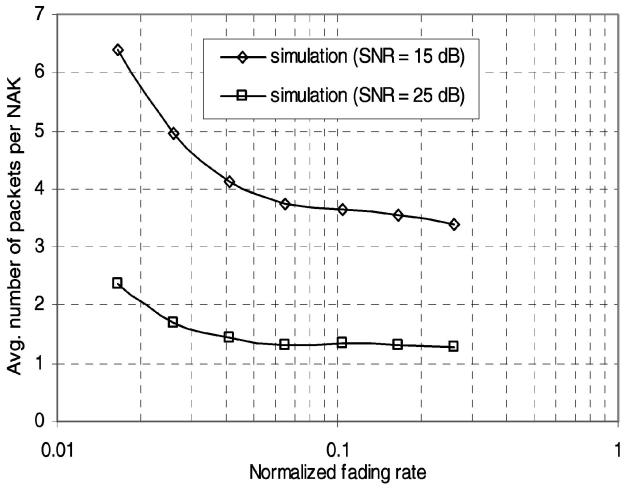

Fig. 11. Average NAK size versus f_dT for $SNR = 15$ dB and 25 dB.

retransmitted per NAK. It is shown in Fig. 10 that the total number of retransmission increases as f_dT increases, but the average number of packets retransmitted per NAK decreases, as shown in Fig. 11. These results reveal the cause of goodput drop in the random-error environment. The increase of the normalized fading rate causes the channel errors to occur more random. Therefore, a fewer number of packets is in retransmitted groups but more number of retransmissions occurs. Because of the round-trip time delay experienced per single retransmission, the goodput decreases as (f_dT) increases.

4.2 Effect of the Channel Delay

Effects of the channel delay on the WAP performance at various values of the normalized fading rate and SNR are studied. Fig. 12 shows the impact of channel delay for $f_dT = 0.02$ (bursty errors) and $f_dT = 0.30$ (random errors). In both cases, we set $N = 30$ and $SNR = 15$ dB. It can be seen that the goodput decreases with the increase of channel delay. This is due to the fact that WAP protocol uses a stop-and-wait mechanism to transmit groups of packets and, thus, the time required to send packet groups gets longer as the channel delay increases. From Fig. 12, it can also be seen that the impact of channel delay on the goodput is higher in random error environment than that in a bursty error environment, and becomes significant as channel delay increases. For instance, when the channel delay is 5ms, the goodput for $f_dT = 0.02$ (bursty errors) is 1,630 bps higher than the goodput for $f_dT = 0.30$ (random error). When the channel delay increases to 55ms the difference in goodput increases to 4,530 bps. This observation can be explained with the results from Section 4.1 where the rate of retransmissions is higher in random errors environment than in a bursty error environment. Since more than twice of the channel delay time is experienced for every retransmission, the goodput is more affected by the channel delay in a random error environment than in a bursty error environment.

4.3 Effect of the SNR

The goodput and efficiency behaviors of WAP are studied by setting $N = 30$, $d = 50$ ms, $f_dT = 0.30$, and vary SNR from 10 dB to 50 dB. Figs. 13 and 14 show the response of

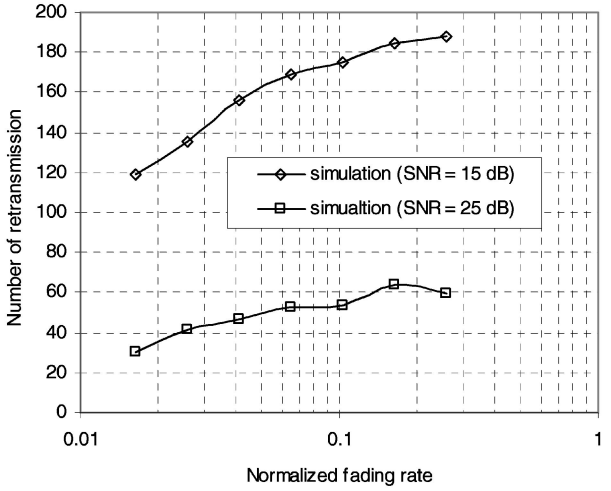

Fig. 10. Number of retransmission versus f_dT for $SNR = 15$ dB and 25 dB.

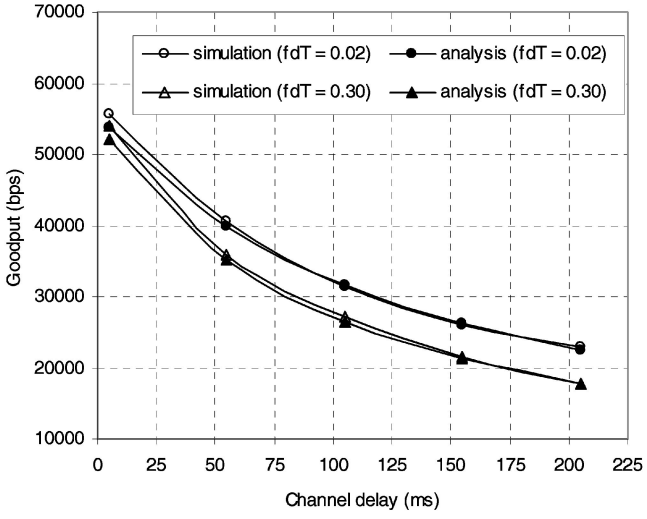

Fig. 12. Goodput versus delay for $f_dT = 0.02$ and 0.30.

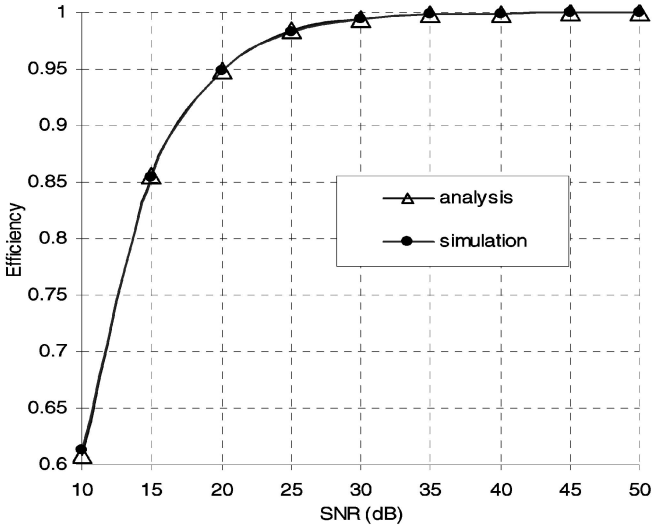

Fig. 13. Efficiency versus SNR.

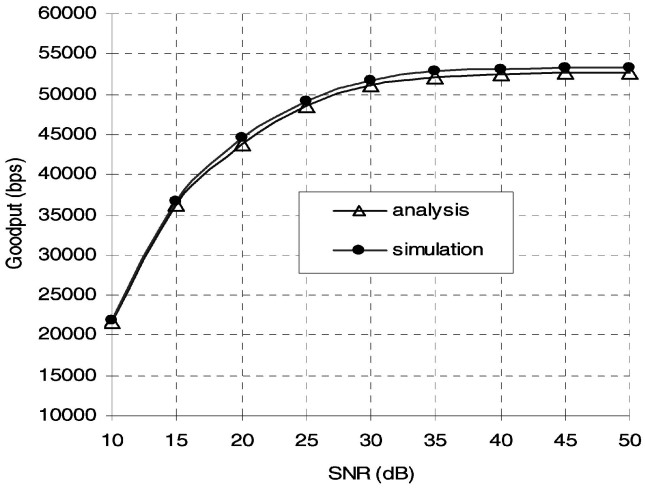

Fig. 14. Goodput versus SNR.

efficiency and goodput to SNR, respectively. It can be seen that the efficiency and goodput increase as SNR increases. As SNR becomes sufficiently large, the goodput and efficiency converge to the limiting points. Appendix B gives the derivation of the upper bounds of the goodput and the efficiency. The upper bound of the goodput is given by

$$\lambda = \frac{N}{(N + 2d)}, \tag{19}$$

where d is the channel delay measured in slots (slot is defined to be the time to transmit one packet), N is the packet group size, and λ is the number of packets per slot. The upper bound of the efficiency is 1. This is because when SNR is sufficient large the PER approaches to zero, and, hence, a perfect transmission (no packet loss). With perfect transmission, the maximum goodput is approximately 53 Kbps from Fig. 14, and 52.7 Kbps from (19).

4.4 Effect of the WAP Packet Group Size

The channel delay degrades the goodput by increasing the proportion of idle time to transmission time. One way of encountering this effect is to increase the size of the transmitted packet group. Fig. 15 shows the effects of WAP packet group size for various channel parameters of particular interest, where $SNR = 20$ dB, $f_dT = 0.02$, $d = 5$ ms, 55 ms, and 155 ms, respectively. It can be seen that as N increases the goodput increases and gradually converges to the limit when N is sufficient large. Also, the value of the WAP packet group size, after which the goodput converges, depends on the channel delay. The reason for these observations is that the increase of packet group size decreases the proportion of idle time to transmission time, which, in turn, increases the goodput. The effects of WAP packet group size in a bursty error environment ($f_dT = 0.02$) and a random error environment ($f_dT = 0.30$) for d = 50 ms, $SNR = 15$ dB are shown in Fig. 16. It can be seen that when $N = 1$, the same goodput is achieved for $f_dT = 0.02$ and for $f_dT = 0.30$. This is due to the fact that when, $N = 1$, all packets are transmitted in a stop-and-wait fashion and, therefore, the correlation of packet losses in a bursty error environment is negligible. When $N > 1$, the goodput in both cases increases as N increases. However, for $f_dT = 0.02$, the goodput increases faster than that for $f_dT = 0.30$. This is because as the WAP packet group size increases, the frequency of group retransmission increases relatively faster in random error environment than in burst error environment.

5 Conclusion

In this paper, the modeling and analysis of WAP performance over wireless links have been studied. Computer simulation results demonstrate that the proposed analytical approach gives a good prediction of the WAP performance over a flat Rayleigh fading channel. It is concluded that WAP protocol performs better in a bursty error environment (channel with memory) than in a random error environment (memoryless channel). The performance of WAP can be improved by increasing the WAP packet group

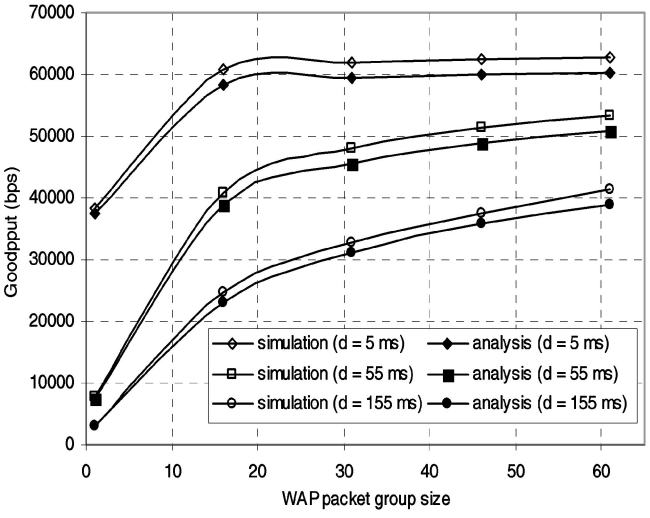

Fig. 15. Goodput versus N for $d = 5$ ms, 55 ms and 155 ms.

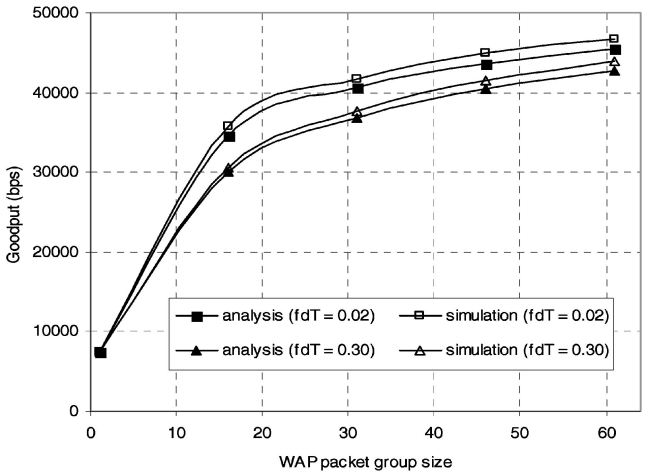

Fig. 16. Goodput versus N for $f_dT = 0.02$ and 0.30.

size, but the range and significance of the improvement depend on the underlying channel settings such as the channel delay, error distribution (or the normalized fading rate), and mean signal to noise ratio.

APPENDIX A
EXPECTED DELAY IN A TRANSIENT PROCESS

Consider a Markov process shown in Fig. 5. Define an indicator variable, $V_{(1,i)'(x,y)'|(0,j)'}(k)$ as

$$V_{(1,i)'(x,y)'|(0,j)'}(k) = \begin{cases} 1, & if\ S(k) = (x,y)' \\ 0, & \text{otherwise} \end{cases}$$

with $S(0) = (1,i)'$ and $S(\infty) = (0,j)'$. Since random variable $V_{(1,i)'(x,y)'|(0,j)'}(k)$ has only two possible values, zero and one, its expected value $\bar{V}_{(1,i)'(x,y)'|(0,j)'}(k)$ is given by

$$\begin{aligned} \bar{V}_{(1,i)'(x,y)'|(0,j)'}(k) &= Pr\{S(k) = (x,y)'|S(0) \\ &= (1,i)', S(\infty) = (0,j)'\}. \end{aligned} \tag{A.1}$$

By Bayes' theorem, we can rewrite (A.1) as

$$\begin{aligned} &\bar{V}_{(1,i)'(x,y)'|(0,j)'}(k) \\ &= \frac{Pr\{S(k) = (x,y)', S(0) = (1,i)', S(\infty) = (0,j)'\}}{Pr\{S(0) = (1,i)', S(\infty) = (0,j)'\}} \\ &= \frac{Pr\{S(\infty)=(0,j)'|S(k)=(x,y)', S(0)=(1,i)'\} Pr\{S(k)=(x,y)'|S(0)=(1,i)'\}}{Pr\{S(\infty)=(0,j)'|S(0)=(1,i)'\}}. \end{aligned}$$

Since

$$\begin{aligned} &Pr\{S(\infty) = (0,j)'|S(k) = (x,y)', S(0) = (1,i)'\} = \\ &Pr\{S(\infty) = (0,j)'|S(k) = (x,y)'\}, \end{aligned}$$

we can proceed with

$$\bar{V}_{(1,i)'(x,y)'|(0,j)'}(k) = \frac{Pr\{S(k)=(x,y)'|S(0)=(1,i)'\} Pr\{S(\infty)=(0,j)'|S(k)=(x,y)'\}}{Pr\{S(\infty)=(0,j)'|S(0)=(1,i)'\}}. \tag{A.2}$$

Let the transmission process start in state $(1,i)'$ and end in state $(0,j)'$. Define a positive random variable $U_{(1,i)'(x,y)'|(0,j)'}$ as the number of times that state $(x,y)'$ is visited, for an infinite number of transitions. Then,

$$U_{(1,i)'(x,y)'|(0,j)'} = \sum_{k=0}^{\infty} V_{(1,i)'(x,y)'|(0,j)'}(k).$$

Assume $U_{(1,i)'(x,y)'|(0,j)'}$ has a finite expected value, the expected number of times that state $(x,y)'$ is visited can be written as

$$\begin{aligned} \bar{U}_{(1,i)'(x,y)'|(0,j)'} &= \overline{\sum_{k=0}^{\infty} V_{(1,i)'(x,y)'|(0,j)'}(k)} \\ &= \sum_{k=0}^{\infty} \bar{V}_{(1,i)'(x,y)'|(0,j)'}(k) \end{aligned} \tag{A.3}$$

since the expectation is a linear operator. Substituting (A.2) into (A.3), we get

$$\bar{U}_{(1,i)'(x,y)'|(0,j)'} = \sum_{k=0}^{\infty} \frac{Pr\{S(k)=(x,y)'|S(0)=(1,i)'\} Pr\{S(\infty)=(0,j)'|S(k)=(x,y)'\}}{Pr\{S(\infty)=(0,j)'|S(0)=(1,i)'\}}. \tag{A.4}$$

By considering a transmission matrix $\mathbf{T} = [t_{(a,i)'(b,j)'}]$ defined by (14), (A.4) can be written as

$$\bar{U}_{(1,i)'(x,y)'|(0,j)'} = \frac{t_{(1,i)'(x,y)'} t_{(x,y)'(0,j)'}}{t_{(1,i)'(0,j)'}}.$$

The expected total number of times, $\sigma_{(1,i)'(0,j)'}$, that transient states $\{(1,1)', (1,2)', (1,3)'\}$ are visited, if the transmission process is started in state $(1,i)'$ and ended in state $(0,j)'$, is computed as

$$\sigma_{(1,i)'(0,j)'} = \frac{\sum_{y=1}^{3} t_{(1,i)'(1,y)'} t_{(1,y)'(0,j)'}}{t_{(1,i)'(0,j)'}}.$$

APPENDIX B
UPPER BOUNDS OF THE GOODPUT AND THE EFFICIENCY

B.1 Analysis of Phase-I Transmission Process

As SNR goes to infinity, the average packet error rate (value of e_i in dominant states) approaches to zero. Then, (10) becomes

$$q_{(a,i)(b,j)} = \begin{cases} p_{ij}, & a = b+1 \\ 0, & otherwise \end{cases} \tag{B.1}$$

for $i,j \in \{1,2,3\}, a,b \in \{1,2,\ldots,N\}$. Consequently, (11) and (12) become

$$\phi^{(I)}_{(a,i)(b,j)} = \begin{cases} p_{ij}(a-1), & a = N, b = 1 \\ 0, & otherwise \end{cases} \tag{B.2}$$

$$m^{(I)}_{(a,i)(b,j)} = \delta^{(I)}_{(a,i)(b,j)} = \begin{cases} (a-1), & a = N \\ 0, & otherwise \end{cases} \tag{B.3}$$

for $i,j \in \{1,2,3\}, a,b \in \{1,2,\ldots,N\}$.

B.2 Analysis of Phase-II Transmission Process

As e_i approaches zero, (13) becomes

$$r_{(u,i)'(v,j)'} = \begin{cases} p_{ij}(2d+1), & u=1, v=0 \\ 0, & otherwise \end{cases} \quad \text{(B.4)}$$

for $i, j \in \{1,2,3\}, u, v \in \{0,1\}$. This equation implies that the system has no transient states and all tapping states have no self-transitions. Therefore, only the first two terms of the summation in (14) are nonzero matrix ($\mathbf{T} = \mathbf{R}^0 + \mathbf{R}^1 = \mathbf{I} + \mathbf{R}$).

$$t_{(u,i)'(v,j)'} = \begin{cases} 1, & u=v, i=j \\ p_{ij}(2d+1), & u=0, v=1 \\ 0, & otherwise \end{cases} \quad \text{(B.5)}$$

From (B.5), (15) can be written as

$$\phi^{(II)}_{(a,i)(b,j)} = \begin{cases} p_{ij}(2d+1), & a=1, b=N \\ 0, & otherwise \end{cases} \quad \text{(B.6)}$$

for $i, j \in \{1,2,3\}, a, b \in \{1,2,\ldots,N\}$. By substituting (B.5) in (17), (17) reduces to one, i.e., $\bar{\sigma}_{(a,i)(0,j)'} = 1$. Therefore, (18) can be rewritten as

$$\delta^{(II)}_{(a,i)(b,j)} = (2d+1) m^{(II)}_{(a,i)(b,j)} = \begin{cases} 2d+1, & b=N \\ 0, & otherwise \end{cases} \quad \text{(B.7)}$$

for $i, j \in \{1,2,3\}, a, b \in \{1,2,\ldots,N\}$.

B.3 Upper Bounds of the Goodput and the Efficiency

From (B.2), (B.3), (B.6), and (B.7), the elements of transition probability matrix, expected transition time matrix, and expected number of transitions, can be found as

$$\phi_{(a,i)(b,j)} = \begin{cases} p_{ij}(2d+N), & a=b=N \\ 0, & otherwise \end{cases} \quad \text{(B.8)}$$

$$\delta_{(a,i)(b,j)} = \begin{cases} 2d+N, & a=b=N \\ 0, & otherwise \end{cases} \quad \text{and}$$
$$m_{(a,i)(b,j)} = \begin{cases} N, & a=b=N \\ 0, & otherwise. \end{cases} \quad \text{(B.9)}$$

By (7) and (B.8) and (B.9), the long-run average goodput λ is given by

$$\lambda = \frac{N \sum_{(N,i)\in W_s} \pi_{(N,i)}}{(2d+N) \sum_{(N,i)\in W_s} \pi_{(N,i)} \sum_{(N,j)\in W_s} \phi_{(N,i)(N,j)}}. \quad \text{(B.10)}$$

From (B.8),

$$\sum_{(N,j)\in W_s} \phi_{(N,i)(N,j)}$$

approaches to one. Therefore, (B.8) reduces to

$$\lambda = \frac{N}{(N+2d)},$$

where d is the channel delay measured in slots (slot is defined to be the time to transmit one packet), N is the packet group size, and λ is the number of packets per slot. With similar arguments, the long-run average efficiency ξ goes to one as SNR approaches to zero.

ACKNOWLEDGEMENT

This work has been partially supported by the Canadian Commonwealth Scholarship and Fellowship Program and by a research grant from the Natural Science and Engineering Research Council of Canada.

REFERENCES

[1] S.A. Karim and P. Hovell, "Everything over IP: An Overview of the Strategic Change in Voice and Data Networks," *BT Technology J.*, vol. 17, no. 2, pp. 24-30, 1999.
[2] Computer Industry Almanac Inc., http://www.c-i-a.com, 2003.
[3] J.F. Kurose and K.W. Ross, *Computer Networking: A Top-Down Approach Featuring the Internet*. Addison-Wesley, 2000.
[4] J. Pan, J.W. Mark, and X. Shen, "TCP Performance and Its Improvement over Lossy Wireless Links," *Proc. IEEE Globecom '02*, pp. 62-66, 2000.
[5] J. Mark, X. Shen, Y. Zeng, and J. Pan, "TCP/IP over Wireless/ Internet Networks," *Proc. IEEE Inter. Conf. 3G Wireless Comm.*, pp. 438-445, 2000.
[6] WAP Forum, "Wireless Application Protocol," http://www.wap forum.org, 1998.
[7] WAP Forum, "Wireless Transaction Protocol Specification," http://www.wapforum.org, 2000.
[8] W.C. Jakes, *Microwave Mobile Communications*, Piscataway, N.J.: IEEE Press, 1993.
[9] E.N. Gilbert, "Capacity of a Burst-Noise Channel," *Bell Systems Technology J.*, vol. 39, no. 9, pp. 1253-1265, 1960.
[10] E.O. Elliott, "Estimates of Error Rates for Codes on Burst-Noise Channels," *Bell Systems Technology J.*, vol. 42, no. 9, pp. 1977-1997, 1963.
[11] M. Zorzi, R.R. Rao, and L.B. Milstein, "On the Accuracy of a First-Order Markov Model for Data Block Transmission on Fading Channels," *Proc. IEEE Int'l Conf. Universal Personal Comm.*, pp. 211-215, 1995.
[12] H.S. Wang and P. Chang, "On Verifying the First-Order Markovian Assumption for a Rayleigh Fading Channel Model," *IEEE Trans. Vehicular Technology*, vol. 45, no. 2, pp. 353-357, May 1996.
[13] H.S. Wang and N. Moayeri, "Finite-State Markov Channel—A Useful Model for Radio Communications Channels," *IEEE Trans. Vehicular Tachnology*, vol. 44, pp. 163-171, 1995.
[14] H.S. Wang and N. Moayeri, "Modeling, Capacity and Joint Source/Channel Coding on Rayleigh Fading Channels," *Proc. IEEE Vehicular Technology Conf.*, pp. 473-479, 1993.
[15] J. Arauz and P. Krishnamurthy, "A Study of Different Partitioning Schemes in First Order Markovian Models for Rayleigh Fading Channels," *Proc. Fifth Int'l Symp. Wireless Personal Multimedia Comm.*, pp. 277-281, 2002.
[16] C. Xion and Y.R. Zheng, "A Generalized Simulation Model for Rayleigh Fading Channels with Accurate Second-Order Statistics," *Proc. IEEE Vehicular Technology Conf.*, pp. 170-174, 2002.
[17] Q. Zhang and S.A. Kassam, "Finite-State Markov Model for Rayleigh Fading Channels," *IEEE Trans. Comm.*, vol. 47, pp. 1688-1692, 1999.
[18] S.M. Ross, *Introduction to Probability Models*, seventh ed. Harcourt, 2000.
[19] R.A. Howard, *Dynamic Probabilistic Systems*. New York: Wiley, 1971.
[20] J.G. Proakis, *Digital Communications*. New York: McGraw-Hill, 1995.

Humphrey Rutagemwa received the BSc degree (with first-class honors) in electronics and communication from the University of Dar Es Salaam, Tanzania, in 1998 and the MSc degree in electrical and computer engineering from the University of Waterloo, Canada, in 2002. He is a PhD student in the Department of Electrical and Computer Engineering at the University of Waterloo. From 1999 to 2000, he was a system engineer at CRDB Bank, Dar Es Salaam, Tanzania. His research interests include end-to-end performance modeling and analysis, QoS provisioning in wireless/IP interworking, and TCP congestion control for multimedia traffic. He is a student member of the IEEE.

Xuemin (Sherman) Shen received the BSc (1982) degree from Dalian Marine University, China, and the MSc (1987) and PhD degrees (1990) from Rutgers University, New Jersey, all in electrical engineering. From September 1990 to September 1993, he was first with Howard University, Washington D.C. and then University of Alberta, Edmonton (Canada). Since October 1993, he has been with the Department of Electrical and Computer Engineering, University of Waterloo, Canada, where he is a full professor. Dr. Shen's research focuses on mobility and resource management in interconnected wireless/wireline networks, stochastic process, and control. He is a coauthor of two books and has publications in communications networks, control, and filtering. Dr. Shen received the Premier's Research Excellence Award (PREA) from the Province of Ontario for demonstrated excellence of scientific and academic contributions in 2003, and the Distinguished Performance Award from the Faculty of Engineering, University of Waterloo, for outstanding contribution in teaching, scholarship, and service in 2002. He serves as a technical vice chair for IEEE Globecom '03 Symposium on Next Generation Networks and Internet, and technical program vice chair for International Symposium on Parallel Architectures, Algorithms, and Networks '03. He is a senior member of the IEEE, and a registered Professional Engineer of Ontario, Canada.